HAL
open science

Evolution of magnetic helicity under kinetic magnetic reconnection: Part II B != 0 reconnection

T. Wiegelmann, J. Büchner

To cite this version:

T. Wiegelmann, J. Büchner. Evolution of magnetic helicity under kinetic magnetic reconnection: Part II B != 0 reconnection. Nonlinear Processes in Geophysics, 2002, 9 (2), pp.139-147. hal-00303034

HAL Id: hal-00303034

https://hal.science/hal-00303034v1

Submitted on 18 Jun 2008

HAL is a multi-disciplinary open access archive for the deposit and dissemination of scientific research documents, whether they are published or not. The documents may come from teaching and research institutions in France or abroad, or from public or private research centers.

L'archive ouverte pluridisciplinaire **HAL**, est destinée au dépôt et à la diffusion de documents scientifiques de niveau recherche, publiés ou non, émanant des établissements d'enseignement et de recherche français ou étrangers, des laboratoires publics ou privés.

Nonlinear Processes in Geophysics (2002) 9: 139–147

Nonlinear Processes in Geophysics
©European Geophysical Society 2002

Evolution of magnetic helicity under kinetic magnetic reconnection: Part II $B \neq 0$ reconnection

T. Wiegelmann[1,2] **and J. Büchner**[2]

[1] School of Mathematics and Statistics, University of St. Andrews, St. Andrews, KY16 9SS, United Kingdom
[2]Max-Planck-Institut für Aeronomie, Max-Planck-Str. 2, 37191 Katlenburg-Lindau, Germany

Received: 1 February 2001 – Revised: 10 April 2001 – Accepted: 17 April 2001

Abstract. We investigate the evolution of magnetic helicity under kinetic magnetic reconnection in thin current sheets. We use Harris sheet equilibria and superimpose an external magnetic guide field. Consequently, the classical 2D magnetic neutral line becomes a field line here, causing a $\boldsymbol{B} \neq 0$ reconnection. While without a guide field, the Hall effect leads to a quadrupolar structure in the perpendicular magnetic field and the helicity density, this effect vanishes in the $\boldsymbol{B} \neq 0$ reconnection. The reason is that electrons are magnetized in the guide field and the Hall current does not occur. While a $\boldsymbol{B} = 0$ reconnection leads just to a bending of the field lines in the reconnection area, thus conserving the helicity, the initial helicity is reduced for a $\boldsymbol{B} \neq 0$ reconnection. The helicity reduction is, however, slower than the magnetic field dissipation. The simulations have been carried out by the numerical integration of the Vlasov-equation.

1 Introduction

Magnetic reconnection due to thin current sheets in sheared magnetic field configurations plays an important role for the dynamics of many space plasma. Examples of plasma configuration with magnetic shear in the solar corona are the boundary between open and closed magnetic field lines in helmet streamers and the heliospheric current sheet. Magnetic shear affects processes where magnetic reconnection is assumed to play an important role: coronal mass ejections (e.g. Low, 1994; Schwenn et al., 1997; Wiegelmann et al., 2000), geo-magnetic substorms (e.g. Birn, 1980) and the interaction of the solar wind with the magnetospheric plasma at the magnetopause (e.g. Song et al., 1995; Otto et al., 1995; Büchner et al., 2001).

An important constraint for possible processes is given by the magnetic helicity. Most solar system plasmas, such as the solar corona or planetary magnetospheres, are almost ideal. In a strictly ideal plasma, the plasma is frozen in the magnetic field and changes in topology are not possible. Thus, magnetic reconnection cannot occur and the magnetic helicity is conserved exactly (e.g. Woltjer, 1960).

A strictly ideal plasma, however, does not exist in nature and thus, magnetic reconnection is possible in principle. It has been conjectured by Taylor (1974) that the helicity is still approximately conserved during the relaxation processes involving magnetic reconnection. Later, Berger (1984) proved that the total helicity is decreasing on a longer time scale than the magnetic energy. In a 2D approach, Vasyliūnas (1975) described reconnection (or magnetic merging) as a plasma flow across a separatrix separating regions of different magnetic connectivity. This implies an electric field perpendicular to the reconnection plane and parallel to the separator, and a localized violation of the ideal Ohm's law. Axford (1984) described magnetic reconnection as a localized breakdown of the frozen-in field condition and the resulting changes in connection as the basis of magnetic reconnection.

The definition given by Vasyliūnas has the drawback of becoming structurally unstable with slight variations of the system. These configurations require a magnetic null line in the reconnection zone. The definition of reconnection by such a magnetic null line is structurally unstable because one can always overlay a finite magnetic field in the reconnection region. A more general definition of magnetic reconnection, including a $B \neq 0$ reconnection, was given by Schindler et al. (1988) and Hesse and Schindler (1988). Within this concept of the so-called general magnetic reconnection, magnetic merging is only a special case with $\boldsymbol{B} = 0$ in the reconnection region, known as a zero-B reconnection. In general, 3D reconnection regions contain a finite magnetic field and parallel electric fields. It was shown that a non-negligible parallel electric field in the reconnection region has global effects. Hence, the total magnetic helicity may change. Hornig (1999) confirmed this result in a covariant formulation, showing that for vanishing $\boldsymbol{E} \cdot \boldsymbol{B}$, the helicity is frozen in a virtual fluid flow of a stagnation type. Ji (1999) investigated magnetic reconnection under the influence of a toroidal magnetic field (guide field) and called this process

Correspondence to: T. Wiegelmann (tw@mcs.st-and.ac.uk)

co-helicity reconnection. He showed that different from a $\boldsymbol{B} = 0$ reconnection (null-helicity reconnection), the helicity becomes dissipated under the influence of a guide field and corresponding parallel electric fields. These investigations, which were all carried out in the framework of magnetohydrodynamics, require a non ideal region, e.g. a resistivity in the reconnection region. The nature of such a resistivity cannot be calculated within MHD and ad hoc assumptions are necessary to prescribe the transport coefficients (e.g. resistivity). The cause of a non ideal behaviour in localized regions of space plasmas is assumed to be anomalous resistivity in thin current sheets. The formation of these thin current sheets can be understood in the framework of MHD (e.g. Schindler and Birn, 1993; Parker, 1994; Wiegelmann and Schindler, 1995; Becker et al., 2001). The further development of these thin current sheets cannot be investigated in the framework of magnetohydrodynamics because their sheet widths become comparable with the ion gyro scale and thus, kinetic effects have to be considered. Furthermore, the MHD investigations cannot predict the local structure of the helicity density in the reconnection zone.

Consequently, the investigation of kinetic effects is necessary to overcome several limitations of MHD, e.g. the necessity of ad hoc assumptions for a resistivity profile, the large limitations of time and length scales compared with kinetic scales, and the impossibility of explaining the local helicity density structure in the reconnection zone. As pointed out by Winglee (1991) in the framework of 2D particle simulations, the generation of a magnetic field component in the current direction (B_y) is a pure particle effect due to the different motion of electrons and ions, as it was predicted by Terasawa (1983). The evolution of B_y changes the helicity density. In 2D, it exhibits a quadrupolar structure after reconnection occurred for pure Harris sheet configurations (Wiegelmann and Büchner, 2001, further cited as paper 1). As predicted by Terasawa (1983), the structure of 2D kinetic reconnection corresponds to a bending of the magnetic field out of the reconnection plane.

The aim of the present paper is the investigation of the kinetic effects in configurations with a finite magnetic field in the reconnection zone, called the $B \neq 0$ reconnection. To do so, we add an additional magnetic guide field $B_{y0} \neq 0$ to the initial equilibrium. The external guide field does not influence the initial Harris sheet equilibria (similar to the MHD case investigated by Seehafer et al., 1996) and is present during the whole simulation run. MHD simulations (Schumacher and Seehafer, 2000) show that a strong guide field suppresses three-dimensionality. This leads to a more strict definition of two-dimensionality, where the system is not only invariant in one spatial direction but, in addition, magnetic and velocity fields have no component in this direction. The rather weak guide field ($B_{y0} < B_0$) used in this paper corresponds to a weaker definition of two-dimensionality, where all quantities are invariant in one spatial direction (y). All vectors (e.g. the magnetic field, currents, flows), however, have three components. Some other authors refer to this approach as $2.5D$.

The paper is organized as follows. In Sect. 2 we outline our simulation approach. Section 3 contains the results of our numerical simulations. We summarize our work in Sect. 4 and give an outlook to future work.

2 Simulation approach

The basic kinetic equations describing the evolution of plasmas is the Vlasov equation:

$$\frac{\partial f_j}{\partial t} + \boldsymbol{v} \cdot \nabla f_j + \boldsymbol{F} \cdot \nabla_u f_j = 0 \tag{1}$$

where $f_j = f_j(x, z, v_x, v_y, v_z)$ is the distribution function and the index j stands for both ions f_i and electrons f_e.

While the full Vlasov equation is six-dimensional, we assume here invariance in one spatial direction (y) which leads us to a five-dimensional equation (3 dimensions in velocity space and 2 dimensions in configuration space).

The Vlasov equations have to be solved self-consistently with the Maxwell equations:

$$\nabla \cdot \boldsymbol{B} = 0, \quad \nabla \cdot \boldsymbol{E} = \sigma,$$
$$\nabla \times \boldsymbol{B} = \boldsymbol{j}, \quad \nabla \times \boldsymbol{E} = -\frac{\partial \boldsymbol{B}}{\partial t}, \tag{2}$$

where $\boldsymbol{B}$ is the magnetic field, $\boldsymbol{E}$ is the electric field, σ is the charge density and $\boldsymbol{j}$ is the current density.

With the help of the magnetic vector potential $\boldsymbol{A}$ and the electric potential ϕ, ($\boldsymbol{B} = \nabla \times \boldsymbol{A}$ and $\boldsymbol{E} = -\nabla\phi - \frac{\partial \boldsymbol{A}}{\partial t}$), we derive the Poisson equations from Maxwell equations:

$$-\Delta \boldsymbol{A} = \boldsymbol{j}, \qquad -\Delta\phi = \sigma, \qquad \nabla \cdot \boldsymbol{A} = 0 \tag{3}$$

The charge density σ and the current density $\boldsymbol{j}$ are calculated by moments of the distribution functions f_i and f_e:

$$\sigma = q_i \int f_i \, d^3v + q_e \int f_e \, d^3v,$$
$$\boldsymbol{j} = q_i \int \boldsymbol{v}_i \, f_i \, d^3v + q_e \int \boldsymbol{v}_e \, f_e \, d^3v.$$

We solve the Poisson equations with the help of an implicit Gauss-Seidel matrix solver. As boundary conditions, we use the Dirichlet boundary conditions in the z-direction:

$$\boldsymbol{A}(x, z_{\min}) = \boldsymbol{A}(x, z_{\max}) = \phi(x, z_{\min})$$
$$= \phi(x, z_{\max}) = 0$$

and periodic boundary conditions in the x-direction. The time integration of the Vlasov equation is carried out by a Leap frog scheme (see paper 1 for details).

Stationary solutions of the Vlasov equation can be found with the help of constants of motion under some constraints, leading to the Grad-Shafranov-equation ($-\Delta A_y = j_y(A_y)$). A well-known equilibrium current sheet solution of the Grad-Shafranov-equation is the Harris sheet profile (Harris, 1962). We use slightly modified Harris-sheet like solutions

(Schindler, 1972) for the initial equilibria. The distribution functions are given by

$$f_j = \rho(x,z) \cdot \exp\left(-\frac{M_i}{2T_i}(v_x^2 + [v_y - u_{dyj}]^2 + v_z^2)\right) \quad (4)$$

$$\rho(x,z) = [1 - \epsilon_1 \cos(2\pi\epsilon_2 x/L)]\frac{1}{\cosh^2(z)} \quad (5)$$

where $\rho(x,z)$ is the density profile and u_{dyj} is the drift velocities. The particle drift in y is necessary in order to produce an electric current and a corresponding magnetic field. An important threshold for kinetic current sheets is the sheet half wide L_z, compared to an ion gyro radius r_i. We use a marginally thin current sheet with $L_z/r_i = 1$. We control L_z/r_i with the ion drift velocity and $L_z/r_i = 1$ requires $u_{dyi} = 2\, v_{\mathrm{Ti}}$.

$\epsilon_1 \ll 1$ in (5) corresponds to a slight variation of the Harris sheet profile in x and $L = 32L_z$ is the simulation box length in x ($-L/2 < x < L/2$ and $x = 0$ in the center of the box). $\epsilon_2 = 2$ corresponds to a sheet with an X-point at $x = 0$ and two O-points at $x = +-L/4$. Let us remark that a constant external magnetic field B_y, pointing in the current direction, does not affect the equilibrium condition of the Harris sheet. The pure Harris sheet $B_y = 0$ can be interpreted as a special case with a shear angle of 180° or opposite magnetic field lines. An external guide field B_{y0} leads, however, to configurations with a shear angle different from the 180° of the pure Harris sheet configurations.

The used simulation parameters are

$x_{\min}/L_z$	-16.0
$x_{\max}/L_z$	16.0
$z_{\min}/L_z$	-4.0
$z_{\max}/L_z$	4.0
Grid points nx	120
Grid points nz	30
Velocity space grid nv	$20 \times 20 \times 20$
X-point location	$x = 0, z = 0$
O-point locations	$x = \pm 8, z = 0$
$\epsilon_1,\ \epsilon_2$ (eqn. 5)	0.05, 2
Mass-ratio M_i/M_e	16
Temperature-ratio T_i/T_e	1
Guide field B_y/B_0	0.2
Time-step $\Delta t/\Omega_{ci}^{-1}$	0.0025
Ion gyro radius r_i/L_z	1.0
used Memory	$1.2GB$
CPU-time (On IBM-RS6000/SP)	$26h$

3 Simulation results

Figure 1 shows the time evolution of the electric field E_y (solid line), and the parallel electric field $E_\parallel$ (dotted line). The dash-dotted line in Fig. 1 shows the reconnected flux between the central X-line ($x = 0, z = 0$) and one O-line ($x = -L/2, z = 0$). After some $6\Omega_{ci}^{-1}$, magnetic reconnection has occurred, and the reconnected flux remains approximately constant. E_y starts decreasing again as a result of the periodic boundary conditions which do not allow additions or removals of plasma from the simulation box. The parallel electric field remains approximately constant after $4\Omega_{ci}^{-1}$. Magnetic reconnection goes along with an electric field. In 2D simulations without an initial magnetic guide field, this reconnection electric field corresponds to E_y which is directed perpendicular to the magnetic field. A significant parallel reconnection electric field does not evolve ($E_\parallel \approx 0$, see paper 1) for initial pure Harris sheet configurations (without guide field B_y). Figures 2f and g show E_y and $E_\parallel$ after reconnection has occurred ($t = 6\Omega_{ci}^{-1}$) for configurations with an initial magnetic guide field investigated in this work. Both E_y and $E_\parallel$ become maximum near the X-points (center X-point at $x = z = 0$ and two X-points at ($x = \pm L/2, z = 0$)), and their magnitudes are comparable ($E_y \approx E_\parallel$). In configurations with an initial magnetic guide field, the electric field component E_y is parallel to the total perpendicular magnetic field B_y (initial guide field plus self-consistent B_y). Consequently, a finite parallel electric field (and a finite $\boldsymbol{E} \cdot \boldsymbol{B}$; see Fig. 2h occurs. In the following, we refer to $t = 6\Omega_{ci}^{-1}$ as the reconnected state.

3.1 Structure of a finite B magnetic reconnection

As in paper 1, we are primarily interested in investigating the helicity evolution, but now for configurations with an initial magnetic guide field. The magnetic helicity can be determined as $H = \int \boldsymbol{A} \cdot \boldsymbol{B} dV$. The total magnetic helicity $H = \int \boldsymbol{A} \cdot \boldsymbol{B} dV$ is gauge invariant (we use the Coulomb gauge $\nabla \cdot \boldsymbol{A} = 0$) for configurations with $\boldsymbol{B} \cdot \boldsymbol{n} = 0$ on the boundary. The latter condition is fulfilled for Harris-like sheet equilibria at the $\pm z_{\max}$ boundaries. With periodic boundary conditions in x, the sheet is unbounded, but cyclic along x. The simulation is invariant in y, i.e. all fluxes are close inside the volume. We diagnose the structure of the magnetic field using the helicity density $h = \boldsymbol{A} \cdot \boldsymbol{B}$. This is analogue to the fluid dynamics helicity density $\boldsymbol{v} \cdot \boldsymbol{\omega}$ which contains important information regarding the flow (see Levy et al., 1990; Moffat and Tsinober, 1992, and paper 1).

To understand the influence of a magnetic guide field on kinetic magnetic reconnection, it is necessary to have some insight regarding the main effects of kinetic reconnection in pure Harris sheet configurations with $B_{y0} = 0$. We have investigated such configurations in paper 1 and briefly summarize the main results here. Due to the different mass of electrons and ions, the mobility is different. Consequently, the particle flux of ions and electrons out of the reconnection zone (X-point) is different (see paper 1, Fig. 3). The ions are streaming primarily parallel to the X-axis, but the electrons are along the separatrices of the magnetic field. The different particle flows cause four ring currents in the wings of the reconnected magnetic field around the central X-point. Each of these currents in the XZ-plane naturally causes a magnetic field B_y perpendicular to the reconnection plane. Due to the orientation of these four currents, the perpendicular magnetic field B_y exhibits a quadrupolar structure. It is relatively weak compared with the lobe field ($B_y \approx 0.03B_0$). In 2D, we have approximately $\boldsymbol{A} \cdot \boldsymbol{B} \approx A_y B_y$ and consequently, the helicity

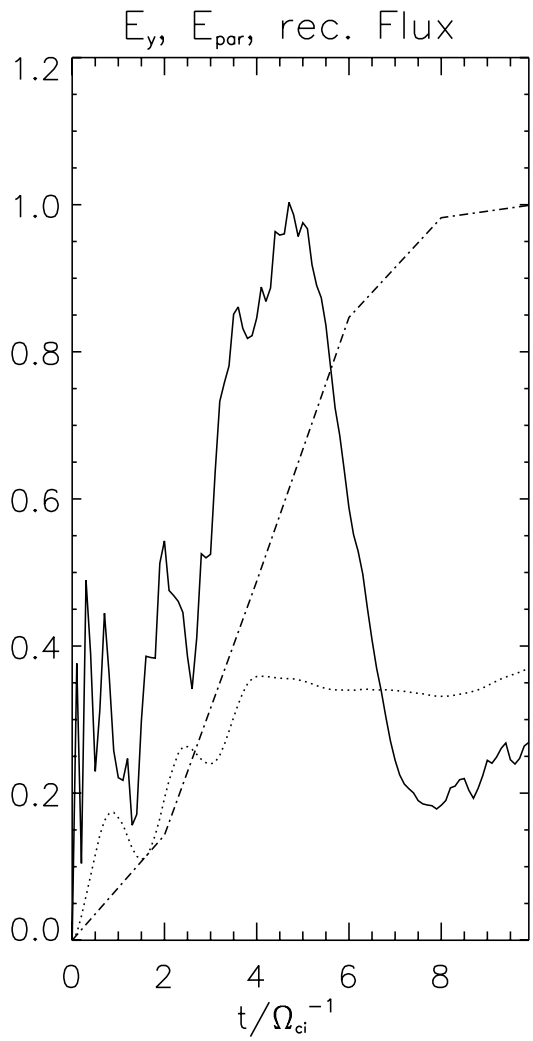

Fig. 1. Time evolution of the electric field components E_y (solid line), and $E_\parallel$ (dotted line) and reconnected flux (dash-dotted line) for $B_{y0}/B_0 = 0.2$. E_y and $E_\parallel$ are averaged over the whole simulation box and normalized to the maximum of E_y. The reconnected flux is normalized to its maximum.

density also contains a quadrupolar structure. The quadrupolar structure of B_y and the helicity density causes a bending of the reconnected magnetic field lines. The O-type field lines are closed (see paper 1, Fig. 4).

What are the consequences of a general kinetic reconnection with an external magnetic guide field? In Fig. 2, we present the following physical quantities for a simulation run with an initial guide field $B_{y0} = 0.2B_0$ after magnetic reconnection has occurred ($t = 6\Omega_{ci}^{-1}$):

(a) Magnetic field component B_y, which is perpendicular to the reconnection sheet (x, z). We present the projection of the magnetic field lines in the reconnection plane as a contour plot of A_y;

(b) Current density projected in the reconnection plane;

(c) Particle flow of the ions projected in the reconnection plane;

(d) Particle flow of the electrons projected in the reconnection plane;

(e) Magnetic helicity density $h = \boldsymbol{A} \cdot \boldsymbol{B}$;

(f) Electric field E_y;

(g) Parallel electric field $E_\parallel = \frac{\boldsymbol{E}\cdot\boldsymbol{B}}{B^2}$

(h) $\boldsymbol{E} \cdot \boldsymbol{B}$.

Figure 2a shows that the initial homogeneous magnetic field B_{y0} developed a structure as the result of kinetic magnetic reconnection. The perpendicular (to the XZ-reconnection plane) magnetic field becomes enhanced locally around the two O-points, which are located at $(x = \pm 8L_z, z = 0)$. While the initially homogeneous magnetic guide field was $B_{y0} = 0.2B_0$, the local maximum of B_y in the center of the O-points is enhanced to $0.4B_0$. Outside the local regions near the two O-points, B_y decreased to a level of $\approx 0.15B_0 \ldots 0.18B_0$. Let us remark that the averaged B_y over the whole simulation box remained constant during the reconnection process.

To understand the physics of this local enhancement of B_y and h, which is different from a $B_{y0} = 0$ reconnection, we investigate the particle flows of electrons and ions (see Figs. 2c and d). Both ions and electrons are accelerated in the reconnection region near the center (X-point at $x = z = 0$). As the electrons are lighter than the ions, their mobility is much higher. The electrons cannot move freely; they are affected by the magnetic guide field B_{y0} and are forced to gyrate in the XZ-plane. The influence of the guide field on the heavier ions is considerably smaller. Instead of being accelerated along the separatrices of reconnection, the gyrating electrons move on rings around the O-points at $x = \pm L/4$ (see Fig. 2b). These ring currents cause a self-consistent perpendicular magnetic field which locally enhances the total perpendicular magnetic field B_y above the level of B_{y0}. As the ring currents around the O-points are primarily produced by the electrons, outside these regions the ion flow becomes more important. The resulting currents cause a considerably smaller perpendicular magnetic field B_y opposite to the initial guide field B_{y0}. Consequently, the total perpendicular magnetic field B_y decreases slightly outside the O-point regions. Notice that the electrons are trapped in the magnetic field near the O-points, which is enhanced due to the above mentioned process.

3.2 Helicity evolution

The local enhancement of B_y leads to a similar local enhancement of the magnetic helicity density h around the O-points (see Fig. 2e). The initial Harris sheet helicity density[1]

$$h(x, z, t = 0) = (\ln\cosh(z_{\max}) - \ln\cosh(z)) \cdot B_{y0}$$

becomes enhanced around the O-points during the reconnection process in accordance with B_y. In the initial state, the

[1] In the initial Harris sheet $\boldsymbol{A}$ contains only the component A_y and consequently $\boldsymbol{A} \cdot \boldsymbol{B} = A_y B_y$

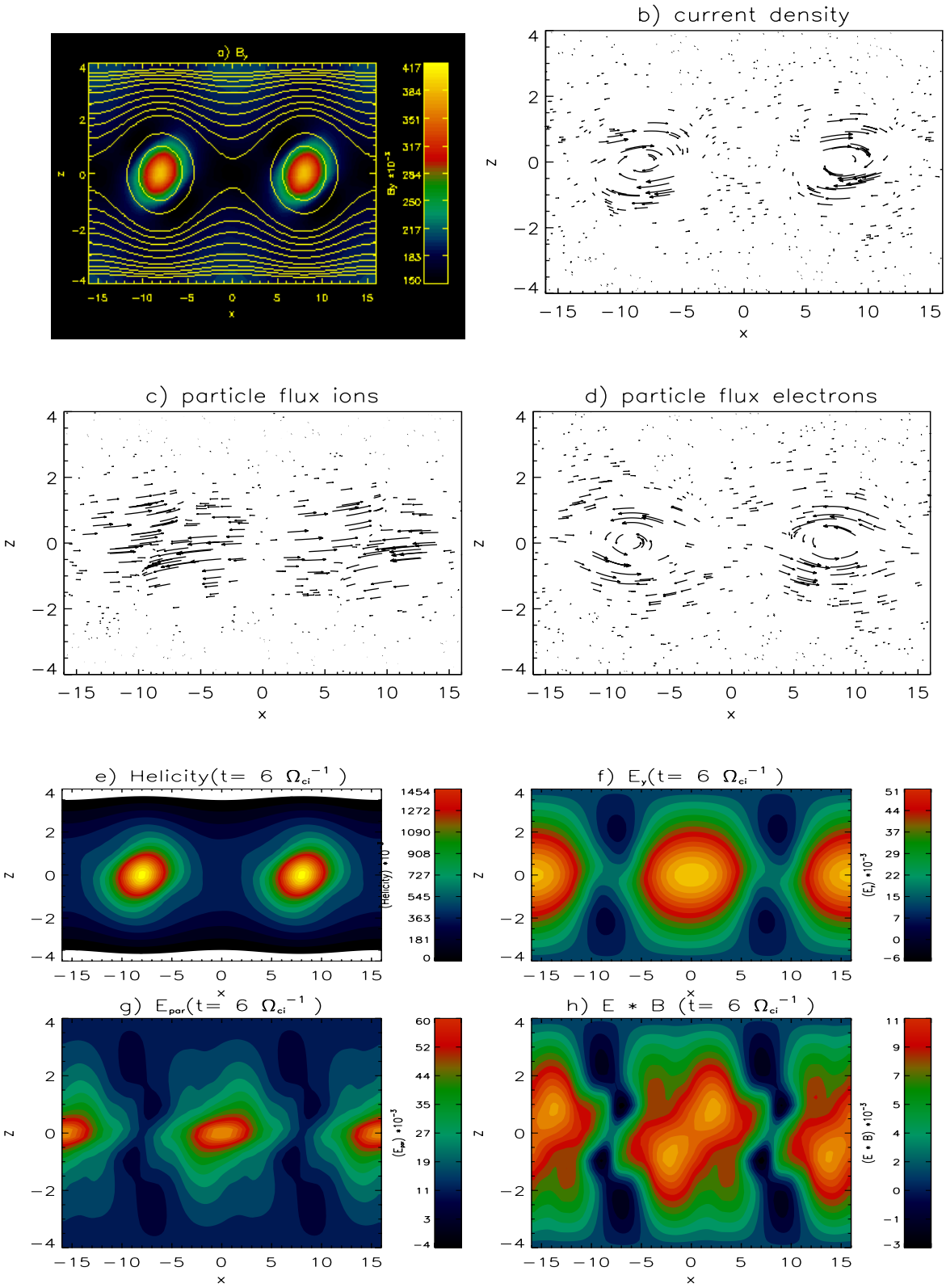

Fig. 2. $\boldsymbol{B} \neq 0$ reconnection, $B_y = 0.2B_0$. **(a)** Contour plot of magnetic field component B_y. The contour lines correspond to a projection of magnetic field lines in the plane. **(b)** Current density. **(c)** Particle flux ions. **(d)** Particle flux electrons. **(e)** Contour plot of magnetic helicity density. **(f)** Reconnection electric field E_y. **(g)** parallel electric field E_{par}. **(h)** $\boldsymbol{E} \cdot \boldsymbol{B}$.

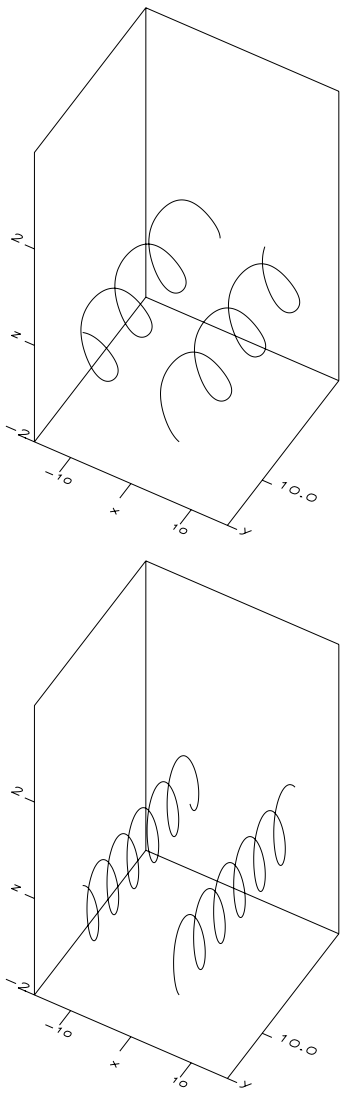

Fig. 3. Enlargement of magnetic field lines for $B_{y0} = 0.2B_0$. The upper panel corresponds to an early state ($t = 2\Omega_{ci}^{-1}$), the lower panel after reconnection has occurred ($t = 6\Omega_{ci}^{-1}$).

helicity has its maximum at the center of the sheet ($h_{0\max} = 0.7B_0L_z$). After reconnection has occurred, the helicity density has its maximum in the center of the O-points. It exceeds (maximum level now $h = 1.4B_0L_z$) by a factor of two the value of the initial state. As the helicity is a measure for the field linkage, this increases by a factor of 2 as well. Figure 3 contains an enlargement of the O-type magnetic field lines at an early state (upper panel, $t = 2\Omega_{ci}^{-1}$) and after reconnection has occurred (lower panel, $t = 6\Omega_{ci}^{-1}$). While we observe a helix with about three and a half convolutions (left-hand side of Fig. 3), the number has increased to five and a half convolutions after reconnection has occurred (right-hand side of Fig. 3). Outside the O-point regions, the helicity density decreased. The averaged helicity density over the whole simulation decreased slightly (see Fig. 1) during the reconnection process.

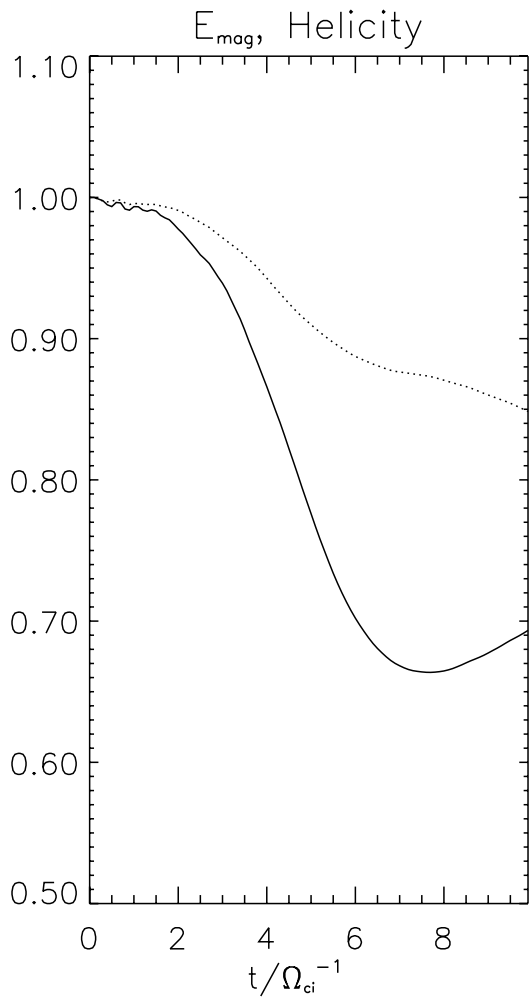

Fig. 4. Time evolution of magnetic energy (solid line) and averaged helicity (dotted line) for $B_{y0}/B_0 = 0.2$.

3.3 Time evolution

Let us compare the evolution of the magnetic energy $E_{\mathrm{mag}} = \int \boldsymbol{B}^2\, dxdz$ (solid line) and the time evolution of the averaged magnetic helicity $H = \int \boldsymbol{A} \cdot \boldsymbol{B}\, dxdz$ (dotted line). In Fig. 4, both values are shown normalized to 1 in the initial state. During the reconnection process, both the helicity and the magnetic energy decreases. The magnetic field is dissipated twice as fast as the magnetic helicity. This faster dissipation of magnetic energy under reconnection has been derived by Berger (1984) in the framework of MHD investigations. Our results confirmed it for the 2D finite $\boldsymbol{B}$ reconnection.

3.4 Influence of the shear angle

Oppositely directed magnetic field lines (pure Harris sheet) correspond to an angle between the field lines of 180°. We refer to this case as pure Harris sheet configurations ($\alpha = 180°$). The results presented so far correspond to a guide field of $B_{y0} = 0.2B_{x0}$. The corresponding shear angle is $\alpha = 180 - 2\arctan(B_{y0}/B_{x0}) = 157.4°$. We also carried

out several simulation runs with different values of B_{y0}/B_{x0}. Here are the results:

- $B_{y0}/B_{x0} = 0.01,\ \alpha = 178.85°$: The very weak guide field cannot trap the electrons. Consequently, Hall currents can still occur, leading to a slightly fuzzy quadrupolar structure in B_y and a helicity density similar to the 180° shear case. But even such a small external B_y causes a helical structure of the reconnected magnetic field lines, contrary to the 180° shear case. The step size in Y of the spiral is very small, but it avoids close circles in O-type field lines;

- $B_{y0}/B_{x0} = 0.04,\ \alpha = 175.4°$: This case is interesting because the external B_y is comparable with the amount of self-consistent B_y due to the Hall-effect in pure Harris sheet reconnection. Here the electrons become already trapped in the guide field. The Hall currents and the corresponding quadrupolar structure in the helicity density and B_y vanish. The main difference of a stronger guide field is the lower step size of the spiral structure;

- $B_{y0}/B_{x0} = -0.04,\ \alpha = 184.6°$: This case reveals the same result as the corresponding case with a positive guide field. The electrons are also trapped in the guide field, but rotate in the opposite direction. Consequently, the evolving ring currents are opposite to the positive guide field case too. The spiral structure has the same step size as in the corresponding positive guide field case, but with the opposite direction;

- $B_{y0}/B_{x0} = 1.0,\ \alpha = 90°$: This very strong guide field does not only trap the electrons, it also forces the ions to gyrate (in the opposite direction as the electrons, of course). Consequently, the ion current contributes to the ring currents as well. The step size of the spiral structure is higher due to the stronger B_y.

4 Conclusions and outlook

In this paper, we investigated the helicity evolution in kinetic reconnection under the influence of an external magnetic guide field ($\boldsymbol{B} \neq 0$ or general magnetic reconnection). We start with a Harris type thin current sheet with a sheet width comparable with the ion gyro radius, to which we add a constant external magnetic field B_{y0}. Such a guide field does not change the Harris sheet equilibrium. Reconnection accelerates ions and electrons out of the X-point region both for $\boldsymbol{B} = 0$ as well as for $\boldsymbol{B} \neq 0$. It is known that in the $\boldsymbol{B} = 0$ reconnection, the accelerated electrons stream freely along the separatrices of the reconnecting magnetic field (see paper 1). This does not occur in the case of the $\boldsymbol{B} \neq 0$ reconnection with an external magnetic guide field B_{y0}. The reason is that the mobility of the electrons becomes reduced because the electrons are trapped in the perpendicular (to XZ-reconnection-plane) magnetic field B_y. The accelerated electrons are trapped in this field and rotate around the B_y direction. Thus, the perpendicular magnetic field reduces the mobility of the electrons. Consequently, the Hall currents, which occur in the $\boldsymbol{B} = 0$ reconnection, do not occur for the $\boldsymbol{B} \neq 0$ reconnection. Instead of these Hall currents, we observe ring currents around the O-lines carried by the electrons (in the XZ-plane). Due to these ring currents, the helicity density and the total magnetic field $B_y(x, z)$ becomes enhanced around the O-lines. This corresponds with the magnetic field becoming helical around the O-points, instead of being bent in the $\boldsymbol{B} = 0$ reconnection case. While the total helicity is conserved for the pure Harris sheet ($\boldsymbol{B} = 0$ reconnection), it becomes slowly dissipated for the $\boldsymbol{B} \neq 0$ reconnection. However, the helicity dissipates slower than the magnetic energy. The slow dissipation of helicity for the $\boldsymbol{B} \neq 0$ reconnection has been investigated by Ji (1999) in the framework of MHD. A difference between the MHD and kinetic $\boldsymbol{B} \neq 0$ reconnection is that in the MHD, the perpendicular magnetic field B_y is not affected by the reconnection process. Due to the different mobility of electrons and ions, Hall currents occur if kinetic effects are considered and contribute to B_y. Table 1 shows the main differences between the kinetic $\boldsymbol{B} = 0$ and $\boldsymbol{B} \neq 0$ reconnection.

Table 1. The main difference between kinetic $\boldsymbol{B} = 0$ and $\boldsymbol{B} \neq 0$ reconnection

	$\boldsymbol{B} = 0$ rec.	$\boldsymbol{B} \neq 0$ rec.
B_{y0}	0	$\neq 0$
Ion flow	Parallel to X-axis	Mainly parallel to X-axis
Electron flow	Parallel to separators of reconnected field	Around B_y
Hall currents	For 4 wings of reconnected field	A ring current around O-lines
B_y-structure	Quadrupolar	O-point structure
Helicity density structure	Quadrupolar	O-point structure
Total helicity	Conserved	Dissipated slowly
O-points	Field lines are closed circles	Field lines are open spirales
$E_\parallel$	$\ll E_y$	$\approx E_y$

In the framework of this work, we neglected any possible structuring of the configuration in the direction of the current flow. This is an appropriate way to investigate the pure effects of the magnetic guide field without perturbation occurring due to instabilities in the current direction (e.g. Büchner and Kuska, 1999). As a next logical step towards a full understanding of kinetic magnetic reconnection under the influence of a magnetic guide field, we plan to take these effects into consideration, leading to 3D simulations in the configuration space (6D in phase space). Several au-

thors pointed out the intrinsic three-dimensional structure of magnetic reconnection in the particle approach (Büchner and Kuska, 1996; Pritchett et al., 1996; Zhu and Winglee, 1996; Büchner, 1999) for Harris sheets with initial anti parallel magnetic field lines. A main difference between 2D and 3D configurations is that in 3D configurations, additional instabilities can occur in the current direction (which is assumed to be invariant in 2D), leading to drift current instabilities and coupled with reconnection (e.g. Büchner, 1999; Wiegelmann and Büchner, 2000). An interesting question is the role of an initial magnetic guide field, i.e. an initial shear angle of reconnecting magnetic field lines different from 180°, for the intrinsic 3D magnetic reconnection process. A basic question which can also be treated in 2D and might be investigated before we concentrate on the full 3D case, is whether the evolution of kinetic current instabilities is affected by a magnetic guide field.

Acknowledgements. We gratefully acknowledge the assistance of H. Michels and I. Silin regarding the optimisation and parallelisation of our Vlasov-Code. We thank T. Neukirch for useful discussions. This work was supported by PPARC and by a visitor grant at the Max-Planck-Institut für Aeronomie in Katlenburg-Lindau. We thank the referees H. Ji and N. Seehafer for their useful remarks.

References

Axford, W. I.: Magnetic field reconnection, in: Reconnection in space and Laboratory Plasma, (Ed) Hones, Jr., E. W., Geophys. Monograph 30, AGU, Washington D. C., 4–14, 1984.

Becker, U., Neukirch, T. and Schindler, K.: On the quasistatic development of thin current sheets in magnetotail-like magnetic fields, J. Geophys. Res., 106, 3811–3825, 2001.

Berger, M. A.: Rigorous new limits on magnetic helicity dissipation in the solar corona, Geophys. Astrophys. Fluid Dynamics, 30, 79, 1984.

Birn, J.: Computer studies of the dynamic evolution of the geomagnetic tail, J. Geophys. Res. 85, 1214, 1980

Büchner, J. and Kuska, J.-P.: Three-dimensional collisionless reconnection through thin current sheets: Theory and selfconsistent simulations in Third International Conference on Substorms (ICS-3), 373, ESA SP-389, October 1996, Noordwijk, The Netherlands, 1996.

Büchner, J. and Kuska, J.-P.: Sausage mode instability of thin current sheets as a cause of magnetospheric substorms, Ann. Geophysicae, 17, 604–612, 1999.

Büchner, J.: Three-dimensional magnetic reconnection in astrophysical plasmas-Kinetic approach, Astroph. and Space Sci., 264, 1/4, 25–42, 1999.

Büchner, J., Nikutowski, B., Kamide, Y., Ogino, T, Otto, A., Poly, P., Korth, A., Mall, U., Vasyliunas, V., Wilken, B., and Woch, J.: Numerical simulation for Cluster tested with Equator-S, ESA-Sp 449, 219–226, 2000.

Harris, E. G.: On a plasma sheath separating regions of oppositely directed magnetic field, Nuovo Cimento, 23,115, 1962.

Hesse, M. and Schindler, K.: A theoretical foundation of general magnetic reconnection, J. Geophys. Res., 93, 5559, 1988.

Hornig, G.: The evolution of magnetic helicity under reconnection, in: Magnetic Helicity in Space and Laboratory Plasmas, (Eds) Brown, M. R., Canfield, R. C., and Pevtsov A. A., Geophysical Monographs Vol. 111, American Geophysical Union, Washington, 157–165, 1999.

Ji, H.: Helicity, Reconnection, and Dynamo Effects, in: Magnetic Helicity in Space and Laboratory Plasmas, (Eds) Brown, M. R., Canfield, R. C., and Pevtsov A. A., Geophysical Monographs Vol. 111, American Geophysical Union, Washington, 167–177, 1999.

Levy, Y., Degani, P., and Seginer, A.: Graphical visualization of vortical flows by means of helicity, AIAA, J. 28, 1347–1352, 1990.

Low, B. C.: Magnetohydrodynamic processes in the solar corona: flares, coronal mass ejections, and magnetic helicity, Phys. Plasmas, 1, 1684–1690, 1994.

Moffat, H. K. and Tsinober, A.: Helicity in laminar and turbulent flow, Ann. Rev. Fluid Mech.24, 281–312, 1992.

Otto, A., Lee, L. C., and Ma, Z. W.: Magnetic field and plasma properties associated with pressure pulses and magnetic reconnection at the dayside magnetopause, J. Geophys. Res., 100, 11 863, 1995.

Parker, E.: Spontaneous Current Sheets in Magnetic Fields, Oxford Univ. Press, New York, NY, 1994.

Pritchett, P. L., Coroniti, F. V., and Decyk, V. K.: Three-dimensional stability of thin quasi-neutral current sheets, J. Geophys. Res., 101, 27 413, 1996.

Schindler, K.: in: Earth's Magnetospheric Processes, (Ed) McCormac B. M., D. Reidel Publ. Comp., Dordrecht, 200, 1972.

Schindler, K. and Birn, J.: On the cause of thin current sheets in the near-Earth magnetotail and their possible significance for magnetospheric substorms, J. Geophys. Res., 98, 15 477, 1993.

Schindler, K., Hesse, M., and Birn, J.: General magnetic reconnection, parallel electric fields and helicity, J. Geophys. Res., 93, 5547, 1988.

Schwenn, R., Inhester, B., Plunkett, S. P., Epple, A., Podlipnik, B., et al.: First View of the Extended Green-Line Emission Corona At Solar Activity Minimum Using the Lasco-C1 Coronagraph on Soho, Solar Phys., 175, 667, 1997.

Schumacher, J. and Seehafer, N.: Bifurcation analysis of the plane sheet pinch Phys. Rev., E 61, 2695–2703, 2000.

Seehafer, N., Zienicke, E., and Feudel, F.: Absence of magnetohydrodynamic activity in the voltage-driven sheet pinch, Phys. Rev., E 54, 2863–2869, 1996.

Song, P., Sonnerup, B. U. Ö, and Thomson, M. F., (Eds): Physics of the Magnetopause, Geophysical Monograph, 90, AGU, Washington D. C., 1995.

Taylor, J. B.: Relaxation of toroidal plasma and generation of reverse magnetic fields, Physical Review Letters, 33, 1139, 1974.

Terasawa, T.: Hall current effect on tearing mode instabilities, J. Geophys. Res. 19 475, 1983.

Vasyliūnas, V. M.: Theoretical models of magnetic field line merging, Rev. Geophys. Space Phys., 13, 303, 1975.

Wiegelmann, T. and Schindler, K.: Formation of thin current sheets in a quasistatic magnetotail model, Geophys. Res. Lett. 22, 2057, 1995.

Wiegelmann, T. and Büchner, J.: Kinetic simulations of the coupling between current instabilities and reconnection in thin current sheets, Non. Proc. Geophys., 7, 141–150, 2000.

Wiegelmann, T. and Büchner, J.: Evolution of magnetic helicity in the course of kinetic magnetic reconnection, Non. Proc. Geophys., 8, 127–140, 2001.

Wiegelmann, T., Schindler, K., and Neukirch, T.: Helmet Streamers with Triple Structures: Simulations of resistive dynamics, Solar Physics 191, 391, 2000.

Winglee, R. M.: Characteristics of the fields and particle acceleration during rapidly induced tail thinning and reconnection, in: Magnetospheric Substorms, Geophys. Monogr. Ser. vol. 64, (Eds) Kan, J. R., Potemra, T. A., Kokubun, S., and Iijima, T., AGU, Washington, D. C., 425, 1991.

Woltjer, L.: On the theory of hydromagnetic equilibrium, Rev. Mod. Phys, 32, 914–915, 1960.

Zhu, Z. W. and Winglee, R. M.: Tearing instability, flux ropes, and the kinetic current sheet kink instability in the Earth's magnetotail: A 3-dimensional perspective from particle simulations, J. Geophys., 101, 4885–4897, 1996.